Electronic Supplementary Material (ESI) for Journal of Materials Chemistry A.

Supporting Information

$CsPbBr_3/Cs_4PbBr_6$ Perovskite@COF Nanocomposites for Visible-Light-Driven Photocatalytic Application in Water

Prachi Kour,[a,b] and Shatabdi Porel Mukherjee*[a,b]

[a]Physical and Materials Chemistry Division, CSIR-National Chemical Laboratory, Dr Homi Bhabha Road, Pune, 411008, India;

[b]Academy of Scientific and Innovative Research (AcSIR), Ghaziabad-201002, India
E-mail: sp.mukherjee@ncl.res.in

Table of Contents

1. Materials

Cesium bromide (CsBr, Sigma-Aldrich, 99%), lead bromide ($PbBr_2$, Sigma-Aldrich, 99%), 1,3,5-triformylphloroglucinol (TFP, Hygeia Laboratories, A.R. grade), ethidium bromide (EB, Sigma-Aldrich,99.9%), 1,4-dioxane (Sigma-Aldrich, 99.8%), mesitylene (Sigma-Aldrich, 99.8%), acetic acid glacial (AA, SRL, extrapure 99.5%), methyl orange (MO, BDH Laboratory Reagent), DMF (AVRA, A.R. grade), hexane (SRL, 99), toluene (SRL, 99%), methanol (Thomas Baker, A.R. grade), triethanolamine (TEOA, Loba Chemie, A.R. 99%), p-benzoquinone (PBZQ, 98+%, Alfa Aesar) and isopropyl alcohol (IPA, SRL, UV and HPLC grade, 99.8%) were used as received without any further purification. Millipore water was used for preparing the solutions and dispersions

2. Experiment:

Synthesis of Ethidium Bromide COF (EB-COF:Br)

The EB-COF:Br was synthesized according to a method previously reported in literature, with slight modifications.[1] In this method, 1,3,5-triformylphloroglucinol (TFP) (0.2 mmol), ethidium bromide (EB) (0.3 mmol), 2 mL 1,4-dioxane‑mesitylene (v/v, 1:1), 0.2 mL of 6M aqueous acetic acid were mixed together at room temperature for 2-3 hours by using DI water as the solvent till a dark brown paste was achieved. This paste was then transferred to a vial and heated in oven at 90°C for 24 hours. The product was then washed thrice with methanol and THF solvents at 60°C for 12 hours each. Finally, the product was dried at 100°C under vacuum for 12 hours to get corresponding EB-COF:Br.

The bulk phase purity of EB-COF:Br was confirmed by powder X-ray diffraction (XRD) measurements. The Brunauer–Emmett–Teller (BET) surface area was calculated from the measured N_2 adsorption desorption isotherm at 77 K for the activated EB-COF:Br at 150 °C in vacuum for 12 h.

Synthesis of $CsPbBr_3$@EB-COF:Br

In a 30 mL glass vial, $PbBr_2$ (3.0 mmol) was dispersed in DMF (10.0 mL), and the mixture was stirred for 30 min at 60°C. Then, the as-prepared EB-COF:Br powder (1 mg/ml) and $PbBr_2$ solutions were mixed and stirred for 2-3 h at 60°C, followed by cooling to RT. The powder was separated by centrifugation under 10,000 rpm for 10 min. The sediment was collected and dispersed in toluene (10 mL). In a separate solution, CsBr (3.0 mmol) was dissolved in MeOH (10.0 mL) at 60 °C. Then, the CsBr/MeOH solution was quickly injected into the $PbBr_2$/toluene precursor solution at 60°C. After 5 minutes of stirring the resulting $CsPbBr_3$@EB-COF:Br composite powder was then centrifuged for 10 min at 10,000 rpm and then washed with hexane twice at 10,000 rpm for 10 minutes. All above operations were performed under ambient atmospheric conditions.

Synthesis of $CsPbBr_3$/Cs_4PbBr_6@EB-COF:Br

The synthetic process was similar to the synthesis of $CsPbBr_3$@EB-COF:Br, but the concentration of $PbBr_2$ and CsBr was 5.0 mmol each.

Synthesis of $CsPbBr_3$-Cs_4PbBr_6without COF:

To synthesize the $CsPbBr_3$/Cs_4PbBr_6 nanocomposite a modified synthesis methodology of the previously reported method was used.[2] Briefly it was as follows, CsBr (1.6mmol) and $PbBr_2$ (0.4 mmol) (CsBr/$PbBr_2$ molar ratio of 4:1) were added to DMF (2 mL) in a centrifuge tube with a volume of 5 mL. The centrifuge tube was ultra-sonicated for 30 min until all the reactants were converted to a light yellowish precipitate. The $CsPbBr_3$-Cs_4PbBr_6 nanocomposite powder was obtained by evaporating the solvent in an oven at 70 °C after centrifugation.

Water stability:

The stability of compounds in water was checked by initially storing the compounds under DI water for a fixed interval of 5, 10, 20, 30, 40, 50 and 60 minutes followed by centrifuge separation and through vacuum drying before analysis.

Photocatalytic experiments:

The photocatalytic performances of the as-synthesized samples were analysed by degradation of Methyl Orange (MO) dye in an aqueous solution under Xe-300W lamp in a Photo catalytic reactor cabinet by Lelesil Innovative Systems. 10 mg of photocatalyst was added to an aqueous solution of MO (10 mL, 20-100 ppm) in a 2 port-quartz reaction vessel at room temperature. The suspended solution was kept in dark for 5 min with continuous stirring to reach an adsorption–desorption equilibrium of MB molecules on the photocatalyst surface. Thereafter, this suspension was irradiated with Xe-300W lamp (λ = 100-1800 nm) and the solution temperature was monitored continuously by a thermocouple and stabilized to 24-26°C to trigger the decomposition of MO molecules under constant magnetic stirring. Aliquots of solution (500 µL) were isolated from the reaction mixture at certain irradiation time and the suspended solids were separated by centrifugation process. The photocatalytic degradation process was monitored by measuring absorption spectrum in the range of 200–700 nm (the maximum absorption of MO at 467 nm) usingUV-1800 Shimadzu spectrophotometer.

For reactions in dark similar method was followed to the light experiments.

3. Characterization:

The phase identification of the as-synthesized samples were performed by Powder X ray diffraction (PXRD), recorded on a Panalytical X'pert PRO powder X-ray diffractometer with Cu Kα radiation.Small Angle X-Ray Diffraction (SAXS) was performed on a Rigaku, Micromax-007HF with highintensity micro focus rotating anode X-Ray generator. The morphologies of the as-synthesised products were investigated using a scanning electron microscope (FEI, ESEM Quanta 200-3D) and High Resolution Transmission Electron Microscope (FEI, Tecnai 20 ST with an accelerating voltage of 200 kV) along with energy dispersive X-ray spectroscopy (EDX) and STEM-HAADF imaging. The HRTEM samples were prepared by drop casting the sample from hexane on carbon-coated copper grids (TED PELLA INC., 200 mesh and SPI, lacey carbon 300 mesh). Thermo-Gravimetric Analysis

(TGA) was performed using SDT Q600 DSC-TGA instrument in Argon atmosphere at ramping rate 10 °C/min. The surface properties of the as-synthesised samples were characterized by X-ray Photoelectron Spectra (XPS) using Thermo Scientific K-Alpha+ X-ray photoelectron spectrometer analyser chamber operating at 2×10^{-7} mbar pressure. Fourier transform infrared (FT-IR) spectra were recorded using Perkin Elmer 2000 FTIR spectrometer in the 400–4000 cm^{-1} region. The Brunauer–Emmett–Teller (BET) surface area of the samples were estimated by the nitrogen gas adsorption–desorption method on a NOVA 1200 (Quantachrome) instrument. UV spectra for all solutions were recorded using UV-1800 Shimadzu spectrophotometer. C, H, N contents were measured using ThermoFinnigan Flash EA1112 Series.

Table S1: The concentration of precursors used to form the respective composites.

Compound	$PbBr_2$	CsBr	COF
$CsPbBr_3$@EB-COF:Br	3 mmol	3 mmol	10 mg
$CsPbBr_3/Cs_4PbBr_6$@EB-COF:Br	15 mmol	15 mmol	10 mg

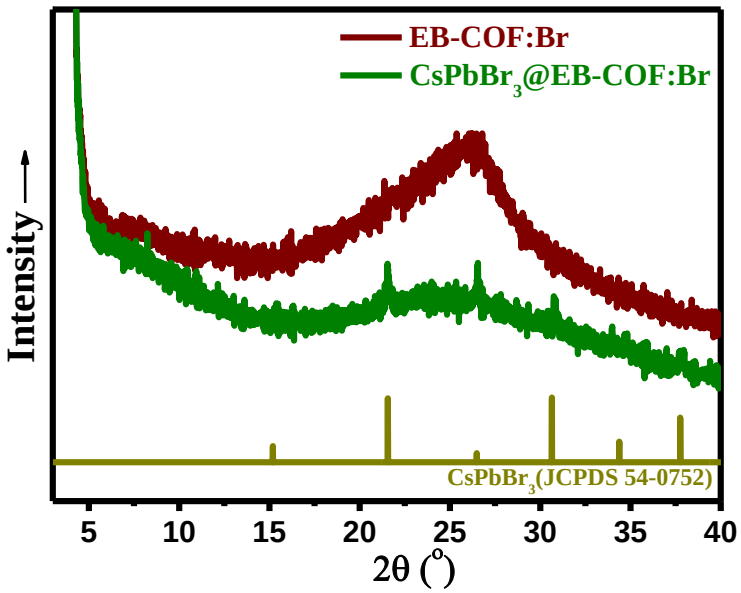

Figure S1: XRD pattern of EB-COF:Br and $CsPbBr_3$@EB-COF:Br (matched with JCPDS no. 54-0752).

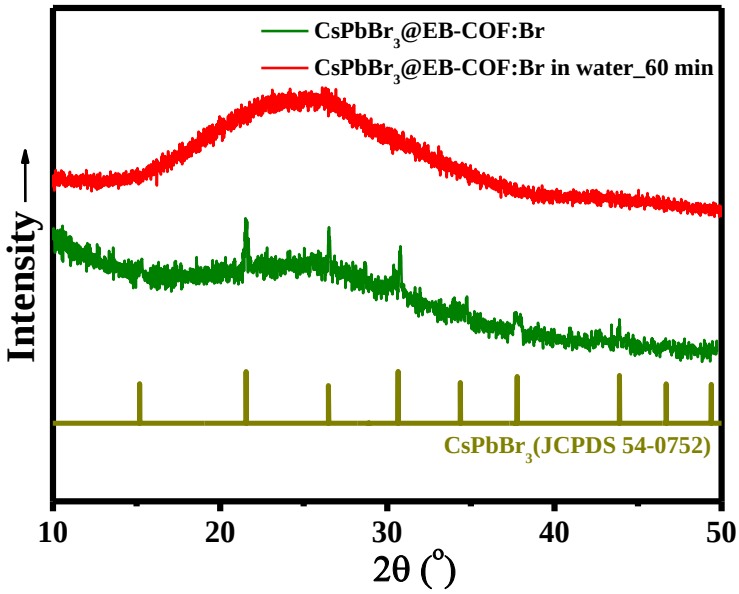

Figure S2: XRD of $CsPbBr_3$@EB-COF:Br compound before and after water stability test for 60 minutes.

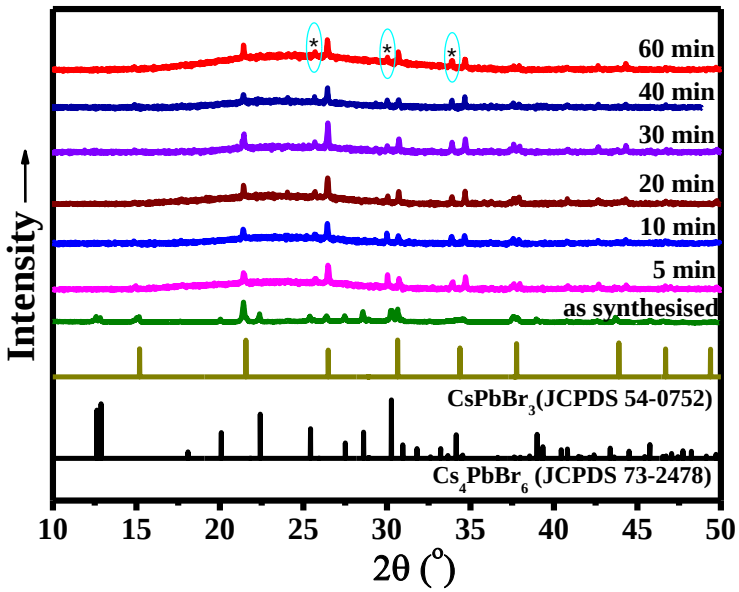

Figure S3: Evolution of XRD with time within the duration of 60 minutes upon water stability test for $CsPbBr_3/Cs_4PbBr_6$@EB-COF:Br compound, matched with JCPDS no. 54-0752 and 73-2478.

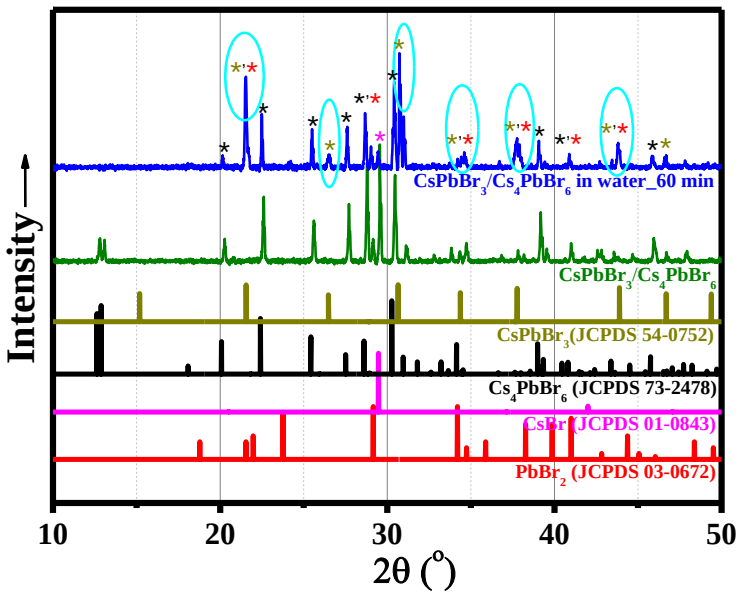

Figure S4: XRD of $CsPbBr_3/Cs_4PbBr_6$ compound before and after water immersion for a duration of 60 minutes followed by vacuum drying before analysis.*

*The XRD shows the appearance of precursor peaks upon water immersion indicating instability of the composite without encapsulation.

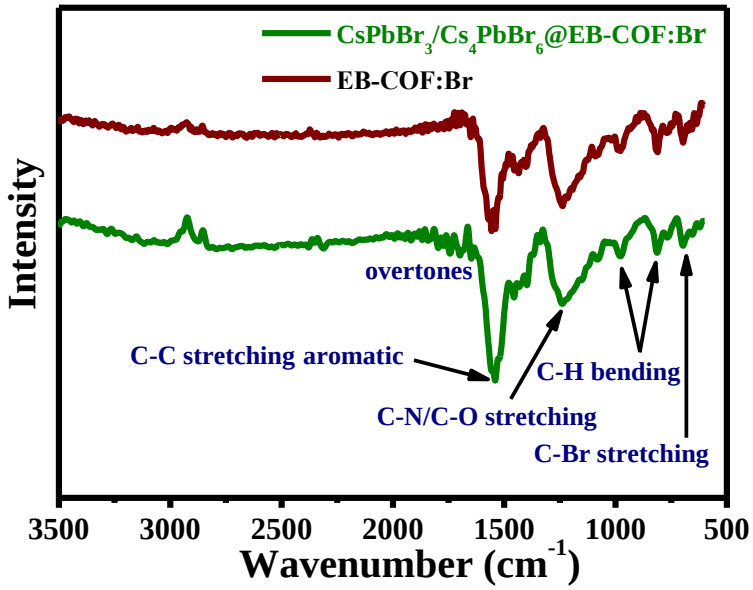

Figure S5: FTIR spectra for EB-COF:Br and $CsPbBr_3/Cs_4PbBr_6$@EB-COF:Br.

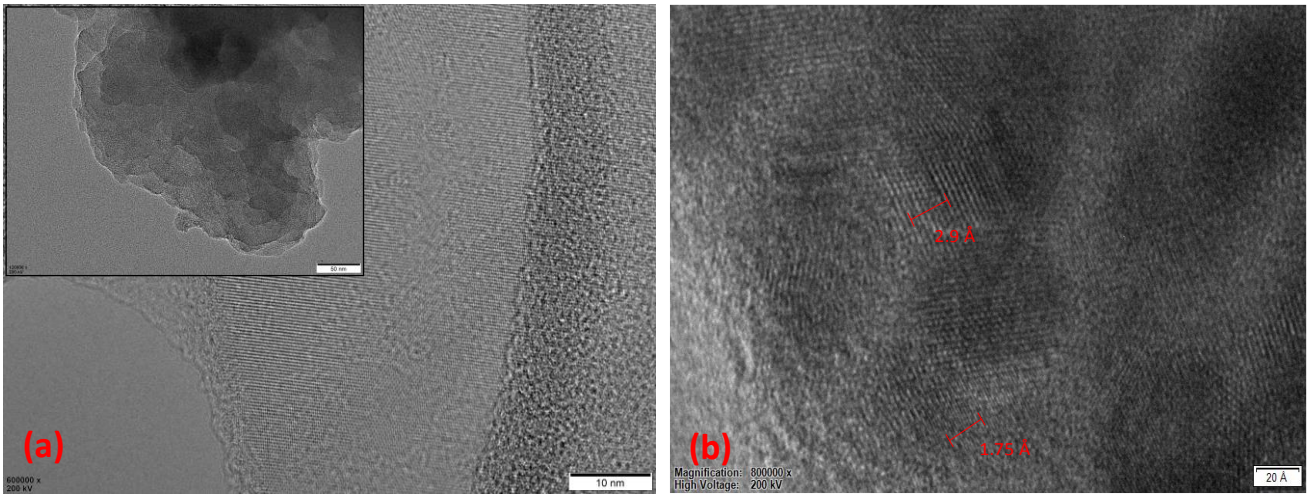

Figure S6: HRTEM images of (a) EB-COF:Br, and (b) $CsPbBr_3/Cs_4PbBr_6$@EB-COF:Br composite showing lattice fringes and the corresponding d-spacing.

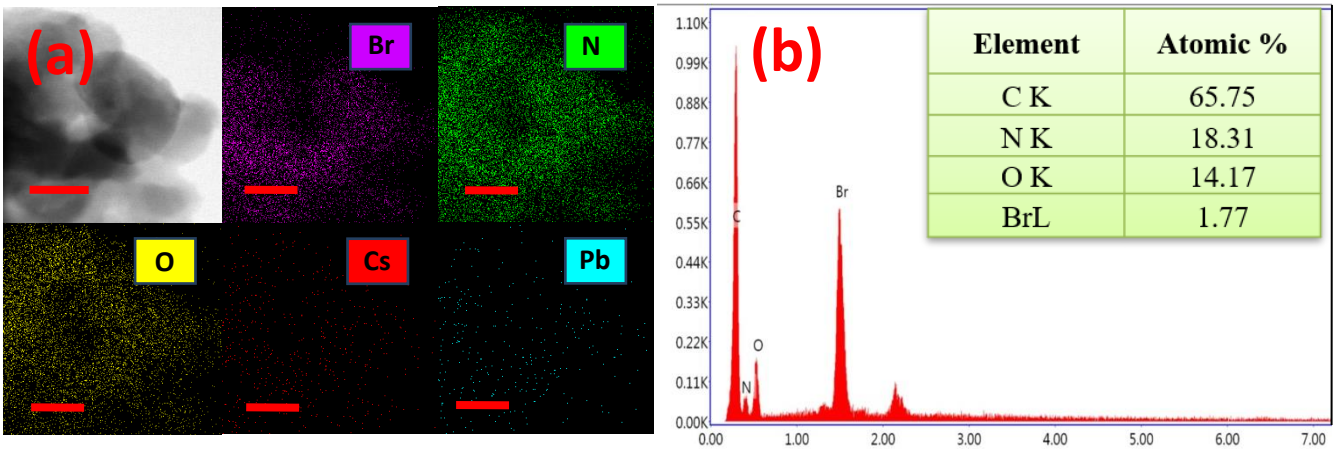

Figure S7: (a) STEM-HAADF mapping for EB-COF:Br (Scale bar = 100 nm) and (b) corresponding EDAX elemental analysis.

Table S2: The C, H and N elemental analysis of EB-COF:Br and $CsPbBr_3/Cs_4PbBr_6$@EB-COF:Br.

Element	C [%]	N [%]	H [%]
Theoretical value of EB-COF:Br[2]	65.06	8.43	4.01
EB-COF:Br	58.82	7.76	4.21
$CsPbBr_3/Cs_4PbBr_6$@EB-COF:Br	38.69	5.40	2.64

The C, H, and N results of the synthesized EB-COF:Br sample show C, N and H content similar to the theoretical value. The calculated C: N: H ratio for synthesized EB-COF:Br was 1: 0.132: 0.072, whereas the ratio from the theoretical value was suggested as 1: 0.139: 0.068. For the sample $CsPbBr_3/Cs_4PbBr_6$ loaded EB-COF:Br, the C: N: H ratio was calculated as 1: 0.129: 0.062. These CHN experiments suggested that the COF structure was remain intact in $CsPbBr_3/Cs_4PbBr_6$@EB-COF:Br composite. Indeed, the EDS elemental analysis of $CsPbBr_3/Cs_4PbBr_6$@EB-COF:Br composite shows the presence of Pb and Br in excess quantity (Cs: Pb: Br = 1:1.53:5.65), further confirming the existence of $CsPbBr_3/Cs_4PbBr_6$ NCs inside EB-COF:Br cavities along with the elemental mapping.

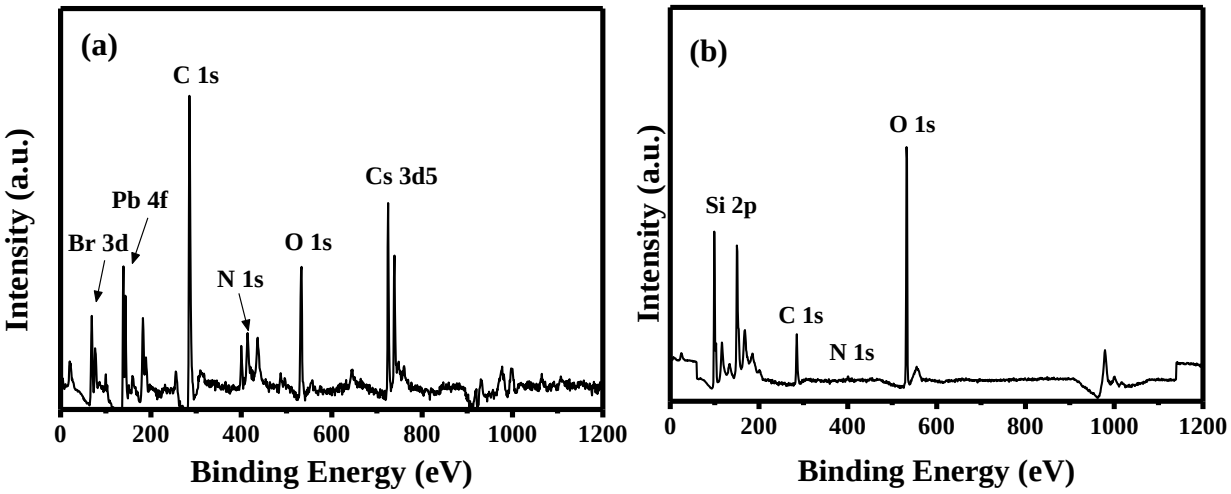

Figure S8: XPS survey scan (a) $CsPbBr_3/Cs_4PbBr_6$@EB-COF:Br and (b) EB-COF:Br.

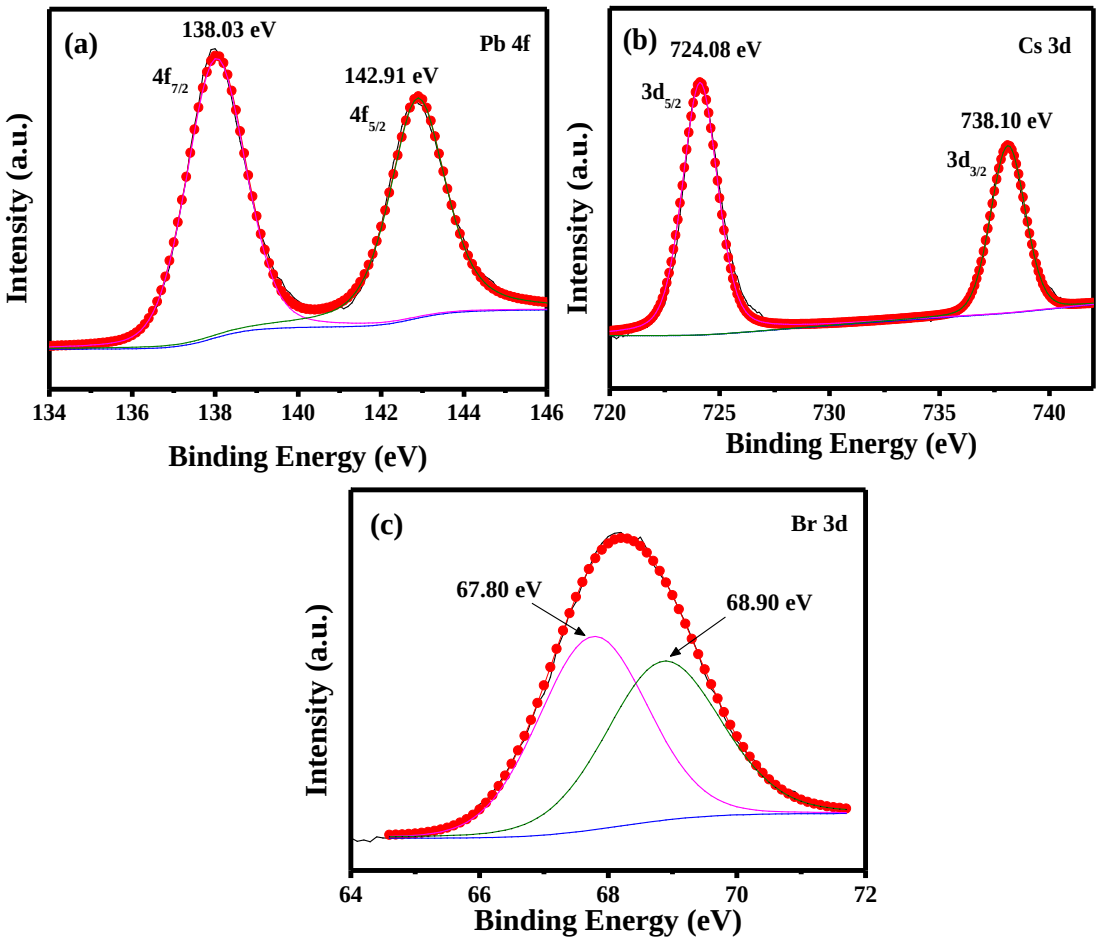

Figure S9: XPS spectrum of (a) Pb 4f, (b) Cs 3d and (c) Br 3d for $CsPbBr_3/Cs_4PbBr_6$@EB-COF:Br.

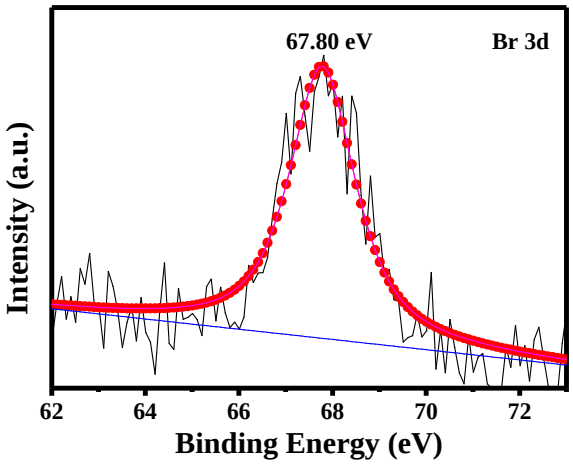

Figure S10: XPS spectrum of Br 3d for EB-COF:Br.

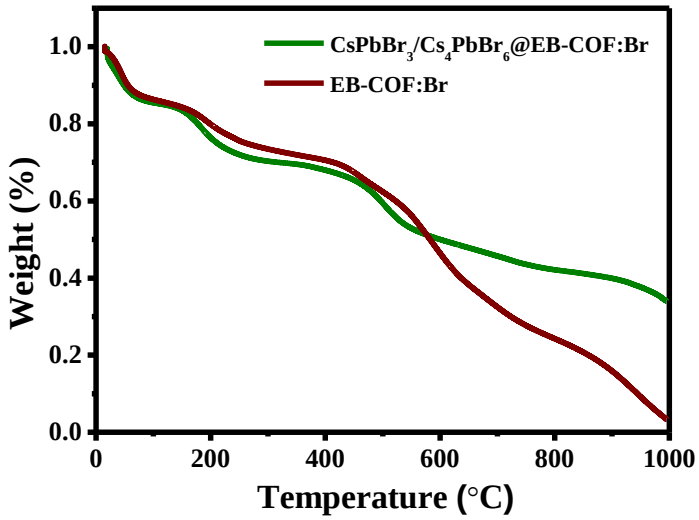

Figure S11: Comparative TGA for EB-COF:Br and $CsPbBr_3/Cs_4PbBr_6$@EB-COF:Br nanocomposite.

Table S3: Table for calculated photodegradation rate constant, κ using formula $C=C_0e^{-\kappa t}$ (first order kinetics)

MO photodegradation condition	Rate constant (min^{-1})
No photocatalyst (in light)	5.995E-4
EB-COF:Br (in dark)	0.018
EB-COF:Br (in light)	0.057
$CsPbBr_3/Cs_4PbBr_6$@EB-COF:Br (in dark)	0.014
$CsPbBr_3/Cs_4PbBr_6$@EB-COF:Br (in light)	0.245

Table S4: Comparative literature survey on degradation rates of organic pollutants under the action of different halide perovskite nanocatalysts to show the excellence of the $CsPbBr_3/Cs_4PbBr_6$@EB-COF:Br nanocomposite photocatalyst reported to date.*

Sr. No.	Photocatalyst	Light Source	Concentration and Volume of Dye Solution	Dye used	Degradation Time (minutes)	Efficiency / Rate constant	Reference
1.	$CsPbBr_3/Cs_4PbBr_6$ @EB-COF:Br (10 mg)	300W Xenon lamp	100 ppm (10 ml)	MO	25	0.245 min^{-1}, 100%	This Work
2.	$CH_2NH_3SnI_3$ (80 mg)	300W Xenon lamp	10 ppm (80 ml)	Rhodamine B (RhB)	50	0.0066 min^{-1}, 40%	3
3.	$CsPbBr_3$ NCs (1 mg)	500W Xenon lamp	10 ppm (3 ml)	MO	100	89%	4
	$CsPbCl_3$ NCs (2 mg)					90%	

4.	$CsSnBr_3$ (120 mg)	1 Sun Simulator ($1kW/m^2$)	2 ppm (100 ml)	Crystal Violet Blue	120	73.1%	5
5.	$CH_2NH_3PbBr_3$@ MOF (2 mg)	LED	~ 18-30 ppm	MO	100	0.027 min^{-1}	6
				Methyl Red (MR)		0.0145 min^{-1}	
		Sunlight		Nitrofurazone		0.0071 min^{-1}	
				MO		0.032 min^{-1}	
6.	$CH_2NH_3PbI_3$ (0.5 mg)	150W Halogen lamp	20 ppm (50 ml)	RhB	180	65%	7
7.	$Cs_3Bi_2Br_9$-OA NCs (7 mg)	Visible light	70 ppm	Methylene Blue (MB)	60	0.69 x 10^{-2} min^{-1}, 26.6%	8
	$Cs_3Bi_2I_9$ – OA NCs (7 mg)					1.8 x 10^{-2} min^{-1}, 62.1%	
8.	$Cs_2AgBiBr_6$ (20 mg)	100 mW cm^{-2} Xenon lamp	100 ppm (10 ml, ethanol)	RhB	120	~ 98%	9
				Rh110		~ 30% - 35%	
				MR			
				MO			
9.	$CsPbI_3$ NCs (0.07 g)	150 W Visible Light	5 ppm (100 ml)	Methyl Violet	120	81.7%	10
				RhB		61.5%	
				Malachite green		42.3%	
				Acid Black 1		33.0%	
				MO		50.8%	
10.	$CsPbBrCl_2$ (20 mg)	500 W Xenon Lamp	~ 3.2 ppm – 5.80 ppm (40 ml)	Eosin B	180	Negligible activity	11
				RhB			
				MO			
				MB			
11.	$TlCdI_3$ (0.005 mg)	125 W mercury lamp	~ 32 - 32.7 ppm	MO	120	27%	12
				MB		100%	
12.	$CsPbBr_3$ NCs (100 mg)	300 W Xenon Lamp	10 ppm (100 ml)	Tetracycline Hydrochloride	30	18%	13
13.	$OHNH_3PbCl_3$, Hydroxyl Ammonium Lead Chloride (20 mg)	Sunlight	5 ppm (40 ml)	Direct Yellow 27	5	82.19	14
	$OHNH_3PbI_2Cl$ (20 mg)				20	93.98	
14	$CsPbI_3$ (20 mg)	500 W Xenon Lamp	5.80 ppm (40 ml)	Eosin B	210	73%	15
	$CsPbBr_3$ (20 mg)					82%	
	$CsPbCl_3$ (20 mg)				140	90%	

*Majorly the concentration of the dye in the water-based photocatalytic reaction were used as 2-5 ppm[5,10,11,14,15], 10 ppm[3,4,13], 20-30 ppm[6,7,12], and 70 ppm[8] and ethanol solution of dye 100 ppm.[9]

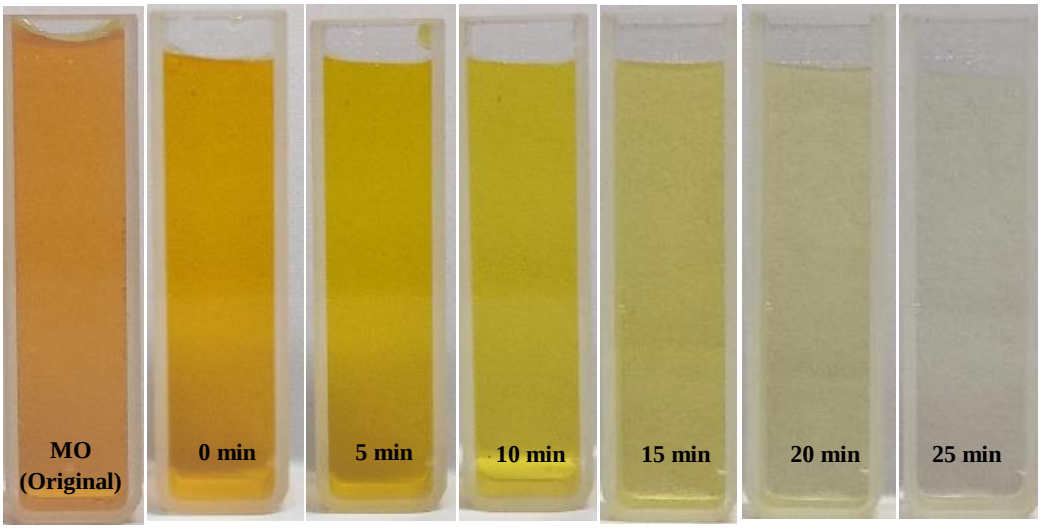

Figure S12: Photographs of 100 ppm MO solutions after photocatalytic degradation as a function of time in presence of $CsPbBr_3/Cs_4PbBr_6$@EB-COF:Br nanocomposite photocatalyst.

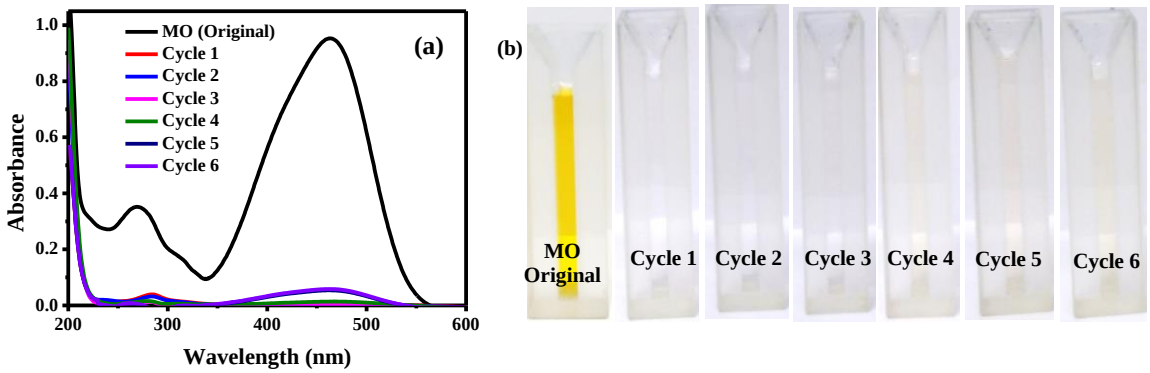

Figure S13. (a) UV-Vis spectra of recycling tests for the photocatalytic degradation for 20 ppm of MO in the presence of $CsPbBr_3/Cs_4PbBr_6$@EB-COF:Br nanocomposite, and (b) photographs of MO solutions after each recycling tests.

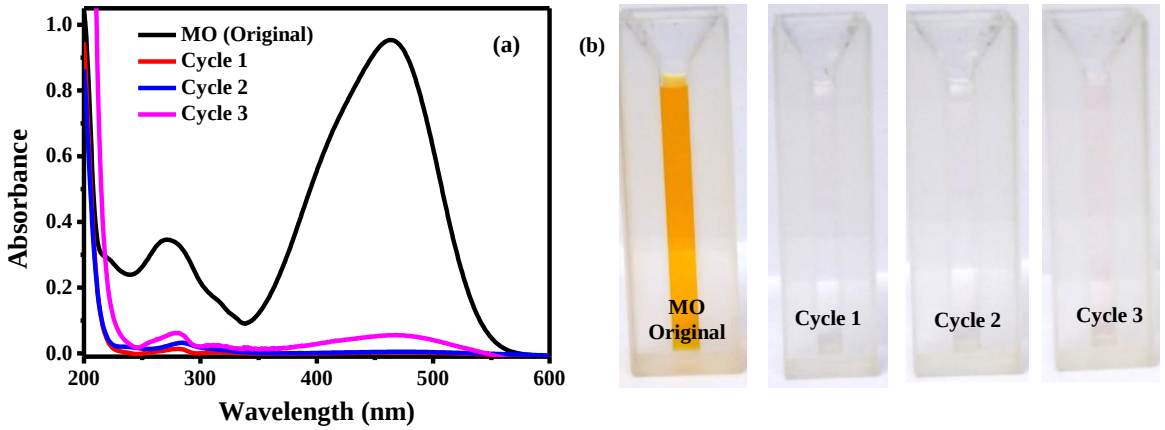

Figure S14. (a) UV-Vis spectra of recycling tests for the photocatalytic degradation for 50 ppm of MO in the presence of $CsPbBr_3/Cs_4PbBr_6$@EB-COF:Br nanocomposite, and (b) photographs of MO solutions after each recycling tests.

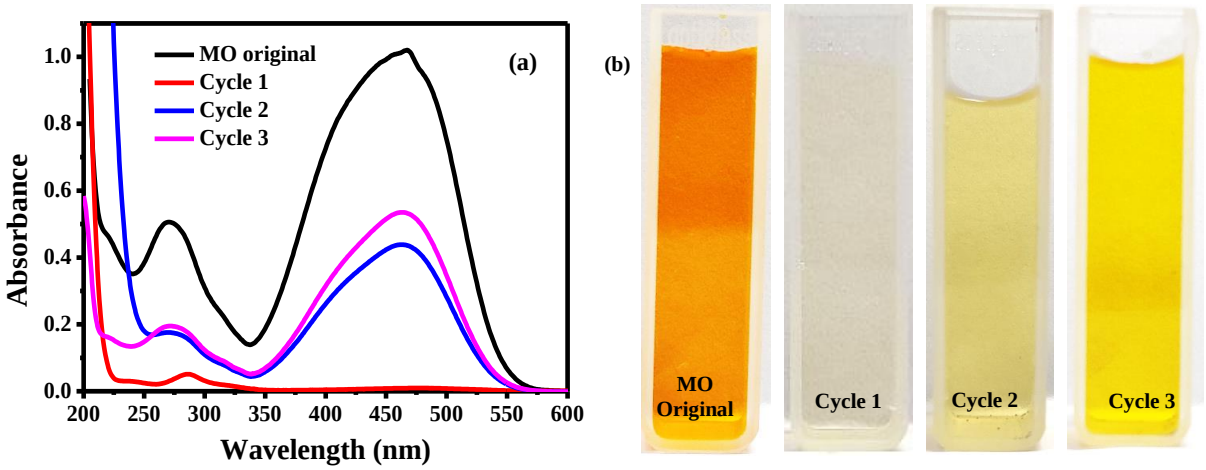

Figure S15. (a) UV-Vis spectra of recycling tests for the photocatalytic degradation for 100 ppm of MO in the presence of $CsPbBr_3/Cs_4PbBr_6$@EB-COF:Br nanocomposite, and (b) photographs of MO solutions after each recycling tests.

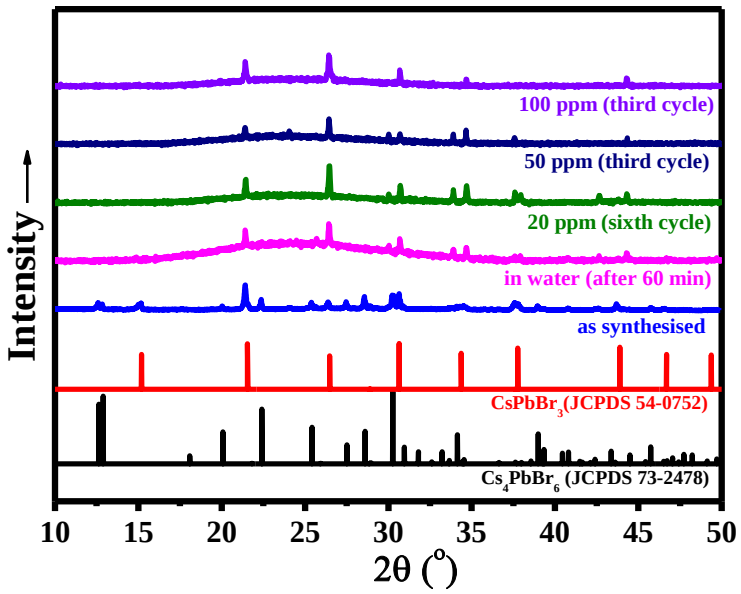

Figure S16. XRD analysis of the photocatalysts ($CsPbBr_3/Cs_4PbBr_6$@EB-COF:Br) after completion of the recycling experiments for 20-100 ppm of MO solution.

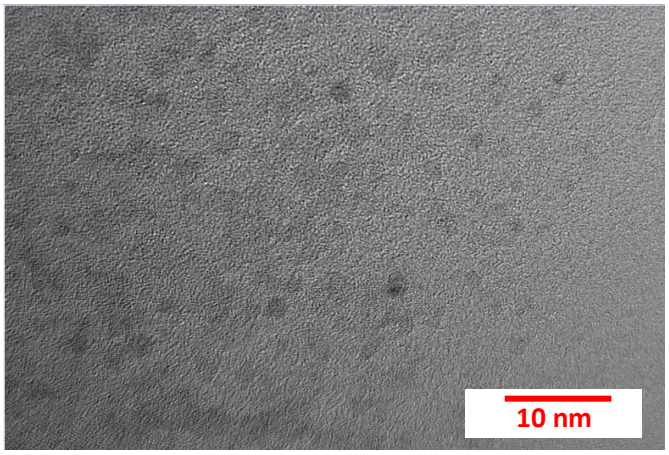

Figure S17: HRTEM image for $CsPbBr_3/Cs_4PbBr_6$@EB-COF:Br nanocomposite after MO recycling experiments of photocatalytic degradation for 100 ppm MO solution.

References

1. H. Ma, B. Liu, B. Li, L. Zhang, Y. G. Li, H. Q. Tan, H. Y. Zang and G. Zhu, *J. Am. Chem. Soc.*, 2016, **138**, 5897–5903.
2. W. Wang, D. Wang, F. Fang, S. Wang, G. Xu and T. Zhang, *Cryst. Growth Des*. 2018, **18**, 6133–6141.
3. W. Zhang, Q. Zhao, X. Wang, X. Yan, J. Xu and Z. Zeng, *Catal. Sci. Technol.*, 2017,

7, 2753–2762.
4. G. Gao, Q. Xi, H. Zhou, Y. Zhao, C. Wu, L. Wang, P. Guo and J. Xu, *Nanoscale*, 2017, **9**, 12032–12038.
5. F. Reyes-Pérez, J. J. Gallardo, T. Aguilar, R. Alcántara, C. Fernández-Lorenzo and J. Navas, *ChemistrySelect*, 2018, **3**, 10226–10235.
6. S. Mollick, T. N. Mandal, A. Jana, S. Fajal, A. V. Desai and S. K. Ghosh, *ACS Appl. Nano Mater.*, 2019, **2**, 1333–1340.
7. B. M. Bresolin, S. Ben Hammouda and M. Sillanpää, *Nanomaterials*, 2020, **10**, 1–17.
8. S. Bhattacharjee, S. P. Chaudhary and S. Bhattacharyya, *ChemRxiv*, 2019.
9. Z. Zhang, Y. Liang, H. Huang, X. Liu, Qi Li, L Chen, and D. Xu, *Angew. Chem. Int. Ed.*, 2019, **58**, 7263 –7267.
10. M. Karamia, M. Ghanbaria, O. Amirib and M. S. Niasaria, *Sep. Purif. Technol.*, 2020, **253**, 117526.
11. T. Paula, D. Dasa, B. K. Dasb, S. Sarkarb, S. Maitic and K. K. Chattopadhyay, *J. Hazard. Mater.*, 2019, **380**, 120855.
12. M. Ghanbari, F. Ansari and M. S. Niasari, *Inorg. Chim. Acta*, 2017, **455**, 88–97
13. X. Qian, Z. Chen, X. Yang, W. Zhao, C. Liu, T. Sun, D. Zhou, Q. Yang, G. Wei and M. Fan, *J. Clean. Prod*, 2019, **249**, 119335.
14. M. Aamir, Z. Hussain, M. Sher and A. Iqbal, *Mater. Sci. Semicond. Process*, 2017, **63**, 6–11.
15. S. Das, T. Paul, S. Maiti and K. K. Chattopadhyay, *Materials Letters*, 2020, **267**, 127501.